Optimization of Spread-Spectrum MSK Sequences and Passive, Multi-Resonant Bandpass Rectifiers for Wireless Power Transfer with Low Electromagnetic Interference

Al-Thaddeus Avestruz, Michael D. Rinehart, and Steven B. Leeb
Department of Electrical Engineering and Computer Science
Massachusetts Institute of Technology
Cambridge, MA 02139
Email: avestruz-at-mit.edu

***Abstract*—This paper addresses the concern for both electromagnetic interference (EMI) and human RF exposure in wireless power transfer (WPT). In many applications like medical, portable, and wearable devices, RF exposure is a greater concern, and the unrestricted ISM bands are often not optimal. Outside of the ISM bands, the restrictions on transmitter power are onerous. The computer-aided design of appropriate spread spectrum sequences to drive WPT and the associated bandpass rectifiers is presented. The sequences are optimized for a new four-quadrant inverse class D amplfier using a genetic algorithm. The wireless power is captured by a high order bandpass rectifier that is optimized using a surrogate model to alleviate the computation cost of performing time domain simulations.**

Keywords*—*Wireless power transfer, spread spectrum, surrogate modeling, bandpass rectifier, minimum shift keying.

I. Introduction

There is a growing concern for both electromagnetic interference (EMI) and human RF exposure in wireless power transfer applications. The conventional solution is to operate in one of the ISM bands such 13.56 MHz or 27.12 MHz [1]–[3] where transmitter power is largely unrestricted. However, in many applications like medical, portable, and wearable devices, where RF exposure of human beings is a greater concern, the ISM bands are often not the optimal frequency [4]–[6]. Outside of the ISM bands, the restrictions on radiated emissions and at lower frequencies, inadvertently conducted emissions, are particularly onerous [4], [7].

A large body of work in power electronics exists in the spectrum spreading of interference using random modulation, which includes [8]–[10] and also in digital clocking [11], [12]. Spread spectrum wireless power transfer requires the power spectrum to be concentrated in the receiver passband with the smallest ratio of the spectral peak to integrated power in the passband. Precise spectral shaping using random methods can be difficult, especially with more complex spectral constraints, with only guarantees of average performance, but not reproducibility. Periodic modulation methods such as frequency sweeping can be precise in spectral shaping, but can introduce sizeable ripple with the same output energy storage because of amplitude modulation from the response of the resonant circuits and because the frequency of this secondary modulation is typically much slower than the base carrier frequency.

The motivation of this paper is to develop methods to increase power delivery while decreasing the peak spectral amplitude of the magnetic field through the use of direct-sequence spread spectrum techniques. From a power electronics perspective, it is desirable to transmit power using a switched-mode as opposed to a linear transmitter and in particular at higher frequencies, a resonant topology with zero voltage switching. We introduce a variant of minimum shift keying (MSK) where the voltage levels are ternary (three-level) with positive and negative half-sine pulses with variable zero durations generated by inverse (or current mode) class D amplifiers (D^{-1}). The application to a classic two-quadrant D^{-1}amplifier is demonstrated, along with a discussion of a new four-quadrant topology that enables a wider spectral spread. The tradeoff is that most of the spread spectrum power is delivered at lower frequencies than the switching frequency, but this is analogous for example to PWM sine wave inverters for motor drives where the design objectives outweigh the tradeoff. The other tradeoff is that during the zero voltage duration in the modulation, no real power is delivered, but current is carried, resulting in additional conduction losses in the transmitter. In applications, such as in biomedical and wearable devices, where receiver efficiency along with low electromagnetic interference is heavily weighted, a tradeoff in transmitter performance (size, complexity, efficiency, or cost) can be appropriate.

To reduce the complexity of the receiver, passive energy conversion through a class of bandpass rectifiers is investigated. Although there is a plethora of work analyzing resonant rectifiers including [13]–[15], which have a resemblance to parts of this bandpass rectifier circuit, together with off-resonance operation and especially with spread-spectrum, where the main difficulty in analysis is that in higher order topologies, multiple diodes are used with inputs that are relatively well-coupled and have outputs which are common. We propose a design method that uses a surrogate model for optimization. Surrogate model optimization has been used for the design of microwave networks [16], [17] and in other engineering disciplines, but has not seen as wide of an

978-1-4799-2147-8/14/$31.00 ©2014 IEEE

application in power electronics.

This paper discusses the numerical optimization of the spreading sequence using a genetic algorithm and the optimization of bandpass rectifiers for spread spectrum.

II. Optimization Based on Standards for Electromagnetic Interference

The magnetic field is proportional within a geometric factor to the total ampere-turns of the wireless power transformer,

$$\oint H \cdot dl = NI = N_p I_p + N_s I_s \tag{1}$$

where I_p and I_s are the primary and secondary currents, respectively, and $N = N_p/N_s$ is the turns ratio. At perfect coupling, $k = 1$, the ampere-turns cancel, but in a near-field wireless charging system where typically $k = 0.01$ to 0.1, most of the flux is uncoupled, representing a finite ampere-turns sum, which is considered spurious. A useful figure of merit is the ratio of the output power P_{out} to the product of the maximum spectral interference,

$$\mathcal{Z} = \frac{N}{k} \frac{P_{out}}{(N_p I_{pf} + N_s I_{sf}) V_{pf}}, \tag{2}$$

where k is the coupling coefficient, and I_{pf}, I_{sf}, and V_{pf} are the peaks in the spectrum of primary and secondary currents and the primary voltage, respectively, at a specified resolution bandwidth (RBW) (e.g. 10 kHz for CISPR11 [4]).

For example, many wireless power receivers use a parallel resonant circuit topology with a transmitter operating at the resonant frequency; for these single-frequency resonant systems, as $Q \to \infty$ for an optimistic bound, $\mathcal{Z} \to 1$. For the same wireless power transformer, a spread-spectrum system does much better, as we show below.

EMI standards typically specify interference limits based on a quasi-peak metric [18] for the spectrum, but the implementation and measurement process is involved and time-consuming. Even a simulated, or approximate version becomes computationally intensive. However, using peak spectral magnitudes in the optimization objective functions is a conservative estimate, which is the approach we apply.

III. Hardware for Resonant Spread Spectrum Power Delivery

A. Power Electronics

We deliver power using ternary (three-level) resonant voltage pulses to a WPT primary inductor as illustrated in Fig. 1d. These pulses are modulated by a modified minimum shift keying (MSK), where the duration of the zero level is variable. MSK is suited for power electronics because the phase modulation occurs at the zero crossings. The classic D^{-1}amplifier and the output waveform is demonstrated in Figs. 1a and 1b, which consist of alternating sine pulses with variable zero durations. A new four-quadrant transmitter based on the D^{-1}amplifier is presented in Fig. 1c. This amplifier operates such that at most only one switch is OFF, which corresponds to a particular phase and sine polarity; during the zero durations, all the switches are ON. A further advantage of this topology is that the power handling is divided among

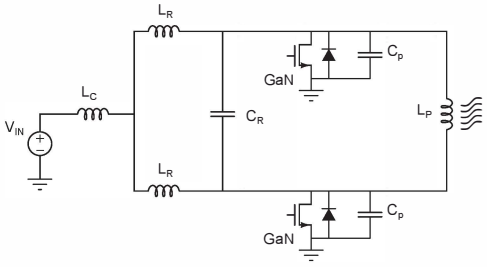

(a) Two-Quadrant

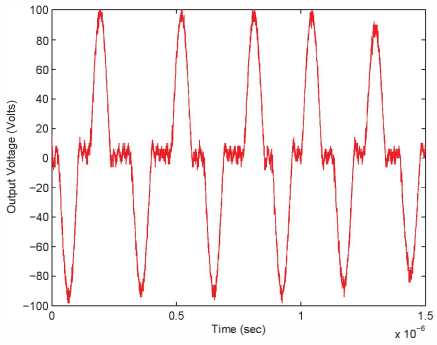

(b) Experimental Output Voltage of Two-Quadrant D^{-1}Amplifier.

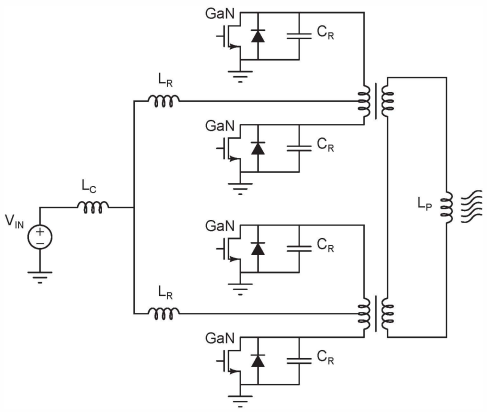

(c) Four-Quadrant

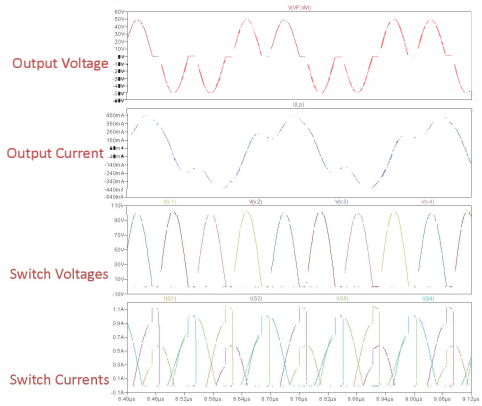

(d) SPICE Simulation of Four-Quadrant D^{-1}Waveforms.

Fig. 1. Inverse Class D Amplifiers

four switches, which improves the power-bandwidth tradeoff for the D^{-1}amplifier. The details of the design of this amplifier will be discussed in a future paper. From the SPICE simulation for an illustrative repetitive pattern in Fig. 1d, the current in the WPT primary L_p is the integral of the amplifier output voltage. Because the input voltage has a spread spectrum, the inductor current is also spread. By explicitly controlling the phase shift of the voltage in a D^{-1}amplifier as opposed to the current in a Class E as in [19], zero voltage switching is always guaranteed.

Spread spectrum power is delivered using an inverse class D (D^{-1}) power amplifier and received by a passive bandpass rectifier. We chose this amplifier for the following reasons:

1) Zero voltage switching for high frequency and/or high voltage operation;
2) Guaranteed zero voltage switching from full load to no load;
3) Tolerance to device removal, i.e. removal of the secondary—guaranteed ZVS; bounded currents and voltages.

B. Digital Control

The transmitter is controlled by a Xilinx Spartan 6 XC8SLX16 FPGA that stores the ternary sequences and zero duration timings to control the power electronics using programmed timers and state machine to determine switching state. The FPGA operates at a clock frequency of 200 MHz, which limits the time resolution of the modulation and hence the WPT operating frequency for this prototype. In a production system, a relatively simple integrated circuit implementation with a triggered ROM or EEPROM to store the modulation encoding, high speed counters, and digital delays would enable operation at higher frequencies.

IV. Optimization Strategy

Several objective functions are possible because both electric field and magnetic field limits may be pertinent depending on EMI standards. This means that objective functions may involve both voltage and current on the primary and secondary WPT inductors. It is worthwhile to note that current is the integral of the voltage across the WPT inductors.

This paper discusses a path towards optimizing a system for wireless power transfer.

1) Find optimal input voltage spectrum and linear system approximation of bandpass rectifier by optimizing together.
2) Optimize t-MSK spread sequence so the spectrum resembles the results from Step 1.
3) Optimize bandpass rectifier so it matches (in the objective function sense) the spectrum from Step 2.

In our application, the possible voltage spectra is constrained in theory by the shape of the pulse (half-sinusoid) and in implementation by the constraints on the inverter. As a strategy, we chose in the sequence optimization to minimize to the peak-to-rms ratio of the primary voltage spectrum; in the design of the bandpass rectifier, to minimize the total amp-turns, which represents the total uncoupled and therefore spurious magnetic field. Other choices are possible, such as a linear weighting on the primary voltage spectrum to minimize the spectral of the current, or perhaps a more complicated objective function. The methods discussed still apply, with maybe higher computational cost.

Optimization was performed using a genetic algorithm followed by a pattern search on the Global Optimization Toolbox in MATLAB. These optimization tools can handle a wider variety of problems including mixed integer and complicated objective functions, which are in general non-convex, yet pertinent for our problem. Although there are no guarantees of finding the global maximum, these tools have been well used in both sequence design in communications [20] and resonant circuits [21], [22].

A. Sequence Optimization Structure

Genetic algorithms and often pattern searches typically require a large number of function evaluations, which also typically increase with the number of optimization variables along with the size of the search space.

While a ternary sequence with fixed zero durations might be optimized directly over $\{-1, 0, 1\}$ because of a smaller search space, it may be advantageous to choose a more efficient representation in optimizing variable zero duration sequences.

If we choose the following representation for an MSK sequence consisting of alternating non-zero $\{-1, 1\}$ and variable zero durations,

$$\{p_1, z_{1,1}, \ldots, z_{1,l}, \ldots, p_n, z_{n,1}, \ldots, z_{n,k}\} \tag{3}$$

where p_i are indices to a dictionary of well-formed subsequences of length k and $z_{i,j}$ are the corresponding zero durations. The subsequences are well-formed in the sense that they satisfy the constraints, for example those imposed by the inverter implementation, or spectral by bounding the run-length of patterns or polarities.

B. Sequence Objective Functions

The objective function used for sequence optimization in this paper minimizes the ratio of the spectral peak to rms power in the signal.

$$\begin{aligned} \underset{x_i, z_{i,j}}{\text{minimize}} \quad & \max_k \quad \frac{W(x_i[n], z_{i,j}[n])}{p(x_i, z_i)} \\ \text{subject to} \quad & x_i \in D \\ & z_{i,j} \in Z_d, \end{aligned}$$

where the objective function is given by

$$W[k] = \left| \mathcal{F}_k \left(\biguplus_i (x_i[n] \amalg z_i[n]) \right) \right| \tag{4}$$

$$p(x_i, z_i) = \frac{n(x_i)}{n(x_i) + \sum_j z_{i,j}}. \tag{5}$$

x_i are subsequences chosen from dictionary D and $z_{i,j}$ are the corresponding constrained zero durations from set Z_d; $z_{i,j}$ are normalized to unity pulse duration. These zero duration constraints may impose minimum and maximum allowable durations, and in the examples discussed below, are integer

multiples of a base duration, which is imposed by the digital controller implementation. For example, the inverter constraints might include volt-second limits, which constrains the possible pulse patterns. $W[k]$ is the magnitude of the discrete Fourier transform $\mathcal{F}_k$ of the sampled time signal formed by the concatenation $\biguplus$ of the time domain construction $\amalg$ of the subsequences with their corresponding zero durations. $p(x_i, z_i)$ is the number of non-zero entries in $W[n]$ added to the sum of zero durations. This is proportional to the signal rms because each half-sine wave pulse has a fixed rms value, so calculating the total portion of time that the pulses occupy is all that is required.

It is important, however, that in the evaluation of the objective function, the peak spectral amplitude that is computed is pertinent. This means that the sampling frequency must satisfy the RBW of the germane EMI standard. For example, CISPR22 with a 10 kHz RBW and a half-sine wave pulse period of 100 ns, requires 10^3 samples per period; this sampling rate is purely for computation of the objective function and should not be confused with an actual implementation in a spectrum analyzer. Another key consideration is that the most efficient algorithm for the discrete Fourier transform is a Fast-Fourier Transform (FFT) on sample lengths which are a power of 2. The typical approach to non-aligned signals is to pad with zeros, but in comparing trial sequences of different lengths, this can bias the estimation and hence comparison of the peak spectral amplitude [23]. One can reduce this estimation bias by over-padding the longest possible sequence by several factors of two so that the ratio of the difference in padding between shortest and longest sequences to the average zero padding is smaller.

For example, in a sequence consisting of 100 ns pulses with zero durations ranging from 15 ns to 100 ns in 5 ns steps, a sequence with 10^3 pulses results in a worst-case sequence period below the RBW of 10 kHz. A fixed sample length which is a power of 2 to accommodate the fastest FFT evaluation is chosen to have an overpadding factor of 4 for the worst-case sequence sample length.

Fortunately, genetic algorithms and pattern searches can be parallelized well. This feature is realized in the Global Optimization Toolbox in MATLAB. The optimizations were performed on a 16-core compute-optimized instance using cloud computing.

C. Sequence Optimization Results

In Figs. 2a and 2c the power spectrum of an equivalent single-frequency sine wave is spread over a two-quadrant and four-quadrant sequence, respectively. Figs. 2b and 2d show the distribution of zero duration.

Fig. 3 shows the progression of the GA optimization, which is typical; the salient feature of this plot highlights the advantage of a GA over a purely random sequence design because even the average population is over factor of two worse than the best GA result for any given generation.

V. Bandpass Rectifier Optimization

There are different ways of receiving spread-spectrum power and converting it to dc; the simplest use passive tuned

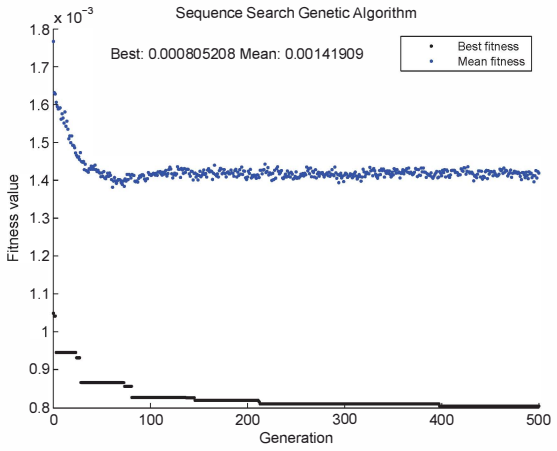

Fig. 3. Genetic Algorithm Optimization

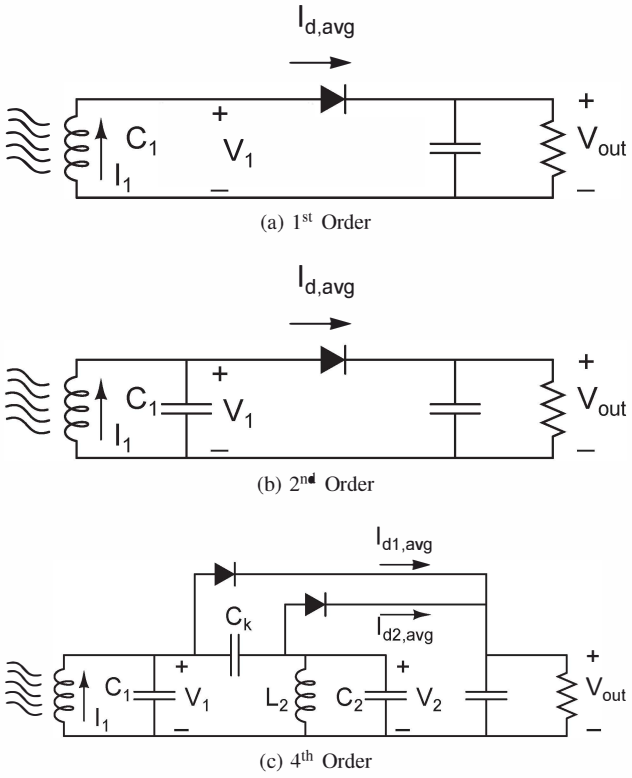

Fig. 4. Bandpass Rectifiers

circuits that are matched to the spread power spectrum. Fig. 4 illustrates several possibilities.

The topologies that require only one rectifier are relatively straightforward in that there is a plethora of work analyzing these types of resonant rectifiers. Although analyses for resonant rectifiers have conventionally been for operation at resonance, based on power balance arguments using the average rectifier current and small enough output voltage ripple, one can also model the rectifier load as a resistor. This results in an optimization of a linear system that can be directly tackled using a genetic algorithm.

When the primary of the WPT transformer is driven by

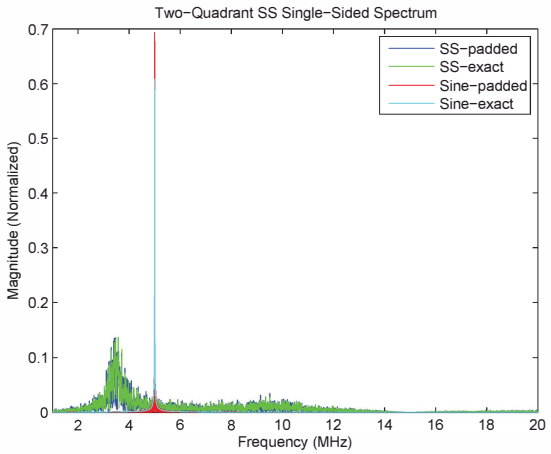

(a) Two-Quadrant Spectrum

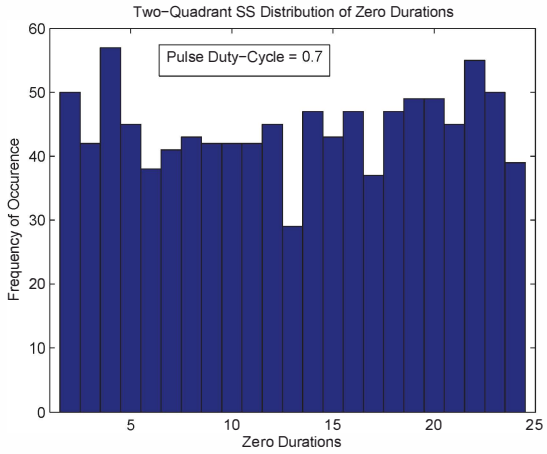

(b) Two-Quadrant Zero Duration Distribution

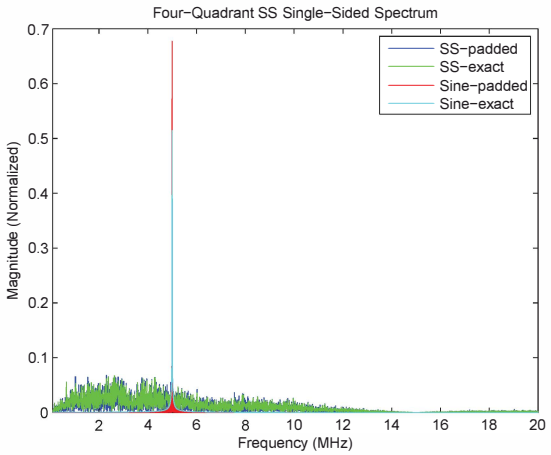

(c) Four-Quadrant Spectrum

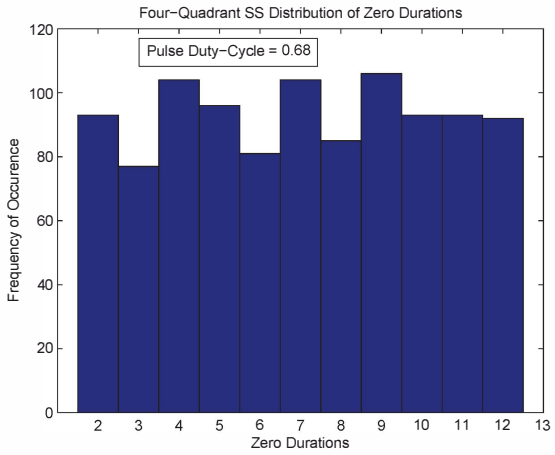

(d) Four-Quadrant Zero Duration Distribution

Fig. 2. Spread-Spectrum Sequence Optimization Results

a voltage source (well-approximated by a D^{-1}amplifier), the output voltage of the WPT secondary is

$$v_2 = \frac{k}{N} v_1 - (1-k^2) j\omega L_2 i_2. \tag{6}$$

This means that we can optimize resonant circuits using a voltage source $V_{in} = V_p k/N$ in series with an inductor $L = (1-k)^2 L_2$ as the input. For small k typical of WPT, L is well-approximated by the secondary inductance L_2.

A. Bandpass Rectifier Optimization Using a Genetic Algorithm

The bandpass rectifiers shown in Fig. 4 are optimized for component values x for a given input voltage v_1 in (6,

$$\begin{aligned} &\underset{x}{\text{minimize}} \quad \max_{\omega} \quad U(\omega, x) \\ &\text{subject to} \quad x_{min} \preceq x \preceq x_{max}. \end{aligned}$$

$$U(\omega, x) = \frac{|NI_p(j\omega, x)| + |I_s(j\omega, x)|}{\sum\limits_{\omega} p(\omega, x)} \tag{7}$$

The optimization seeks to minimize the ratio of sum of the magnitudes of the amp-turns in the WPT transformer to the output power constrained by the bounds on the component values x, e.g. $x = (C_1, C_k, L_2, C_2, R_L)$ in Fig. 4c . By adding the magnitudes of the amp-turns in (7), we optimize for a conservative bound on the amount of spurious field.

The primary current is $I_p = V_1/j\omega L_1$; the secondary current I_s and the point power density $p(\omega)$ is calculated from the direct solution of the mesh equations

$$v = (\mathbf{Z} + r\mathbf{I})i,$$

where r is a real parameter equivalent to a resistance for regularization so the conditioning is bounded over the range of trial component values.

B. Optimizing Input Voltage Spectrum and Bandpass Rectifier Together

A natural question is to ask is if, for a given bandpass rectifier topology, there was an optimal input voltage spectrum v_1 in (6). This requires the simultaneous optimization of both the input voltage spectrum and the component values.

A numerical solver such as a GA is an indispensable tool in optimizing bandpass rectifiers for objective functions of the form in (7). Even for the 2nd order rectifier in Fig. 4a, the analytical approach requires the solution of a non-linear differential equation for the stationary points over ω,

$$\frac{dV_{in}(\omega)}{d\omega}\left(1+\omega^2\tau^2\right) - V_{in}(\omega)\omega\tau^2 = 0.$$

A point-wise optimization of the input voltage spectrum is possible, but computationally intensive because of the number of optimization variables. An alternative would be to optimize over parameters that represent the shape of the spectrum. Fig. 5a shows the results of the optimized unit-normalized input voltage for a 2nd order bandpass rectifier. The input voltage is optimized through the parameterization of the values and locations of the points of a piecewise linear fit; the points reside on a non-uniformly because the optimization naturally places a higher density of points where the features change the most. This results in a good representation of the spectrum for a relatively small number of points. There are upper and lower bounds on the frequency and these are handled by rejecting points outside of the bounds, which works well in practice; a more computationally intensive algorithm is to reflect the points from the boundaries. The signal power in the spectrum is bounded as well.

The optimization results in a fairly flat amp-turns spectrum in Fig. 5b, which is intuitively expected. The resulting output power spectrum is shown in Fig. 5c.

VI. Surrogate Model Optimization for Higher Order Bandpass Rectifiers

Bandpass rectifiers are effectively a matched filter for the power spectrum produced by the transmitter. In Fig.6a, power is extracted from both resonator stages to reduce the circulating currents, especially the first stage which corresponds to current in the receiving coil.

The 4th order bandpass rectifier in Fig. 6a can be approximated by a linear system as shown in Fig. 6b. The equivalent resistances can be found through matching the power balance,

$$\frac{V_o^2}{R_L} = \frac{V_{1,rms}^2}{R_1} + \frac{V_{2,rms}^2}{R_2}. \tag{8}$$

If we let,

$$\begin{aligned} \alpha V_{1,rms}^2 &= V_o^2 \\ \beta V_{1,rms}^2 &= V_o^2, \end{aligned} \tag{9}$$

we can parameterize the resistances by the relationship between the rms voltages and the dc output voltage,

$$\begin{aligned} \frac{1}{R_L} &= \frac{1}{\alpha R_1} + \frac{1}{\beta R_2} \\ &= \frac{1}{R_1'} + \frac{1}{R_2'}. \end{aligned} \tag{10}$$

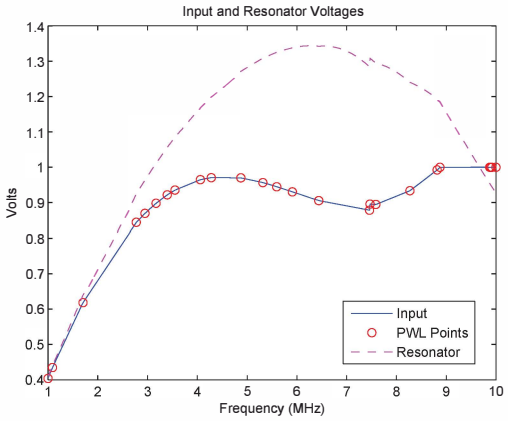

(a) Input and Resonator Voltages

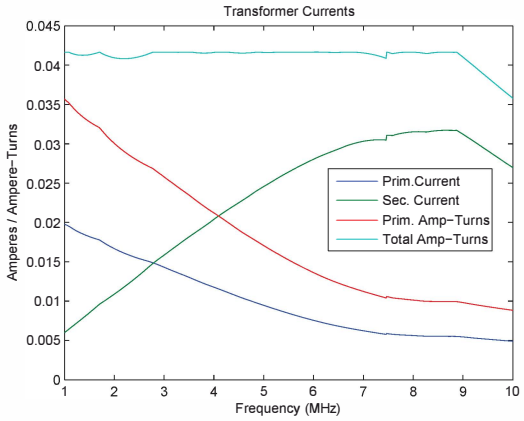

(b) Winding Currents and Ampere-Turns

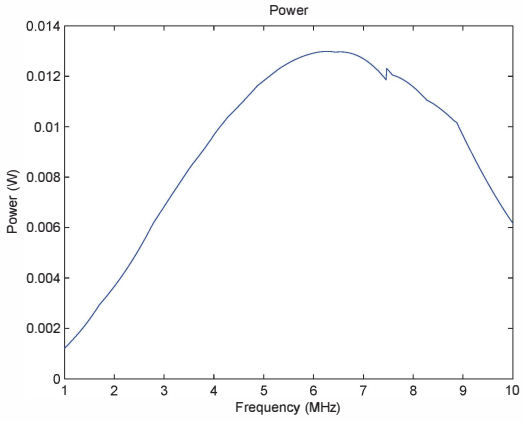

(c) Output Power Spectrum

Fig. 5. Frequency Sweep of Linear Model of 2nd Order Bandpass Rectifier Optimized for the Input Spectrum and Component Values Simultaneously.

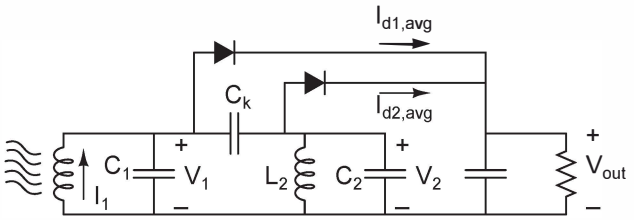

(a) Time Domain Nonlinear Rectifier Model

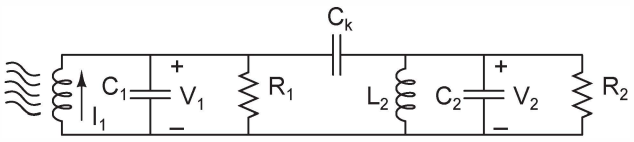

(b) Frequency Domain Surrogate Linear Model

Fig. 6. Surrogate Modeling for a 4th Order Bandpass Rectifier

If we parameterize the effective resistances in terms of the load resistance R_L,

$$\begin{aligned} &\gamma_1 R_1' = R_L \\ &\gamma_2 R_2' = R_L \\ &\quad \Rightarrow \qquad\qquad \gamma_1 + \gamma_2 = 1, \end{aligned} \tag{11}$$

then

$$\begin{aligned} \hat{R}_1 &= \frac{\hat{R}_L}{\alpha\gamma_1} \\ \hat{R}_2 &= \frac{\hat{R}_L}{\beta\gamma_2}, \end{aligned} \tag{12}$$

hence

$$\begin{aligned} \gamma_1 &= \frac{i_{d1,avg} R_L}{V_o} \\ \gamma_2 &= \frac{i_{d2,avg} R_L}{V_o} \end{aligned} \tag{13}$$

and

$$\begin{aligned} \alpha\gamma_1 &= V_o i_{d1,avg} / \frac{V_{1,rms}^2}{R_L} \\ \beta\gamma_2 &= V_o i_{d2,avg} / \frac{V_{2,rms}^2}{R_L}. \end{aligned} \tag{14}$$

The optimization can be described as follows:

1) Perform initial GA optimization on surrogate model for unconstrained $\hat{R}_1$ and $\hat{R}_2$ to find the closest R_L.
2) Use GA optimization results C_1, C_k, L_2, C_2, and R_L to run a nonlinear time domain simulation of the real system. R_L can be derived from $\hat{R}_1$ and $\hat{R}_2$ in (10).
3) Use steady-values for $\{V_o, V_{1,rms}, V_{2,rms}, i_{d1,avg}, i_{d2,avg}\}$ to derive the parameters $\{\alpha, \beta, \gamma_1, \gamma_2\}$.
4) Run GA optimization for $\{C_1, C_k, L_2, C_2, R_L\}$ using $\{\alpha, \beta, \gamma_1, \gamma_2\}$ to solve for $\{R_1, R_2\}$ in the objective function.
5) Goto step 2 until stopping criterion is reached, e.g. $\mathcal{Z}$ non-decreasing.

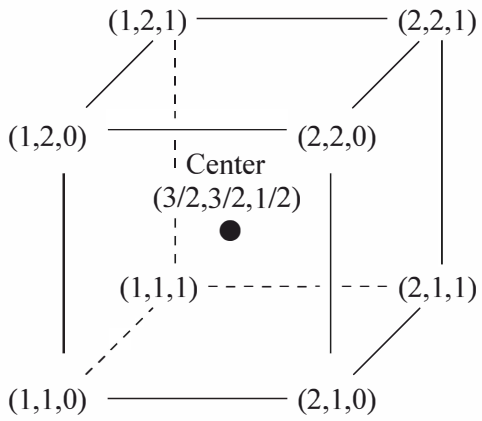

Fig. 7. Starting Volume of Valid R_L Over $(\alpha, \beta, \gamma_1)$ Parameterization

A. Initial R_L

The optimization starts by finding the optimal vector of component values in the surrogate model using a genetic algorithm. The component values are constrained by practical considerations such as component size, parasitics, and perhaps by some other heuristics. The inductors in our example are constrained to be between 30 nH and 1 μH, the capacitors between 30 pF and 1 nF, and the resistors between 10 Ω and 10 kΩ. Within these bounds, the relationship between R_1 and R_2 are unconstrained.

We proceed to a time domain simulation of the actual nonlinear system to find the R_L that results in the closest (in the 2-norm sense) R_1 and R_2 to the surrogate model. We perform a grid search using parallel simulations in the $(\alpha, \beta, \gamma_1)$ parametric space for R_L, where

$$R_L = \frac{1}{2}\left(\alpha\gamma_1 R_1 + \beta\left(1-\gamma_1\right) R_2\right) \tag{15}$$

from (11) and (13). From physical considerations, $0 \leq \gamma_1, \gamma_2 \leq 1$. The lower bound $\alpha, \beta \geq 1$ is the case for V_1 and V_2 being square waves in (9). A pattern search [24] can also be performed using the box illustrated in Fig. 7 as the starting point, where $\alpha, \beta = 2$ corresponds to sinusoidal V_1 and V_2.

B. Example Optimization Results

The results for a trial input voltage are show in Fig. 8; a wider frequency range for power capture is possible for higher order bandpass rectifiers. Higher order bandpass rectifiers allow the quality factors (Q) of the individual coupled resonators to be higher for a given bandwidth with multiple rectifiers allowing power to be captured at every stage, adding degrees of freedom with which to reduce the current in the WPT receiver inductor.

VII. Experimental Results

A wireless power transfer system consisting of spiral wound inductors (3.4 μH primary and 1 μH secondary) driven by a two-quadrant D^{-1}amplifier is shown in Fig. 9. The

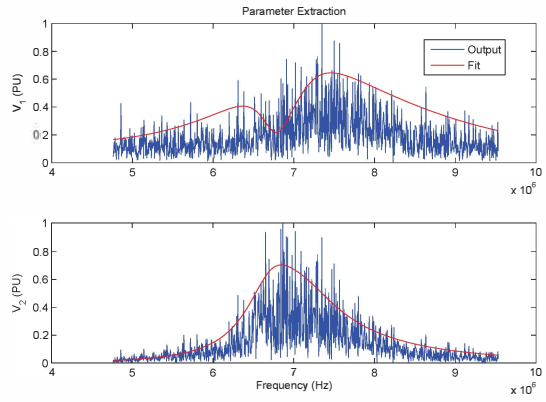

(a) Spectrum of V_1 and V_2

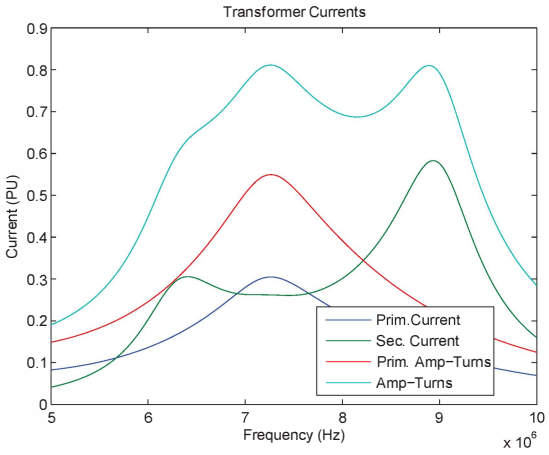

(b) Inductor Currents and Amp-Turns

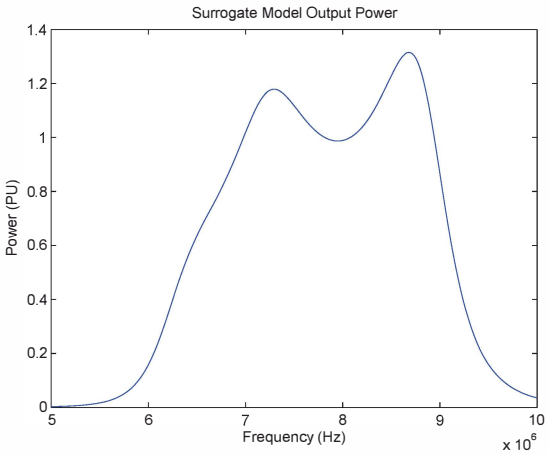

(c) Surrogate Model Output Power Spectrum

Fig. 8. Fourth-Order Bandpass Rectifier Optimization Results

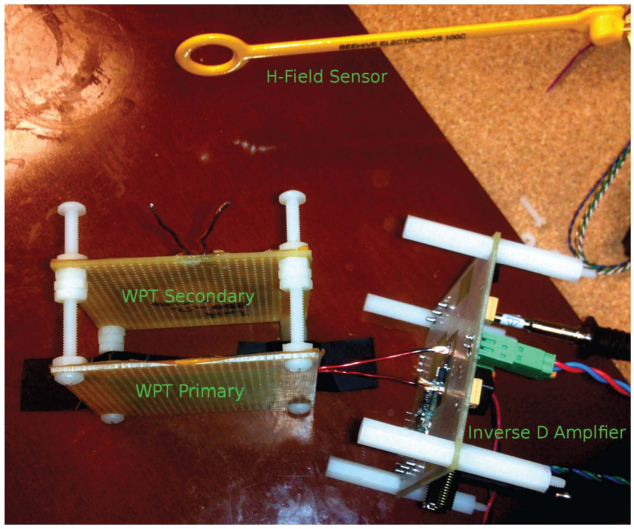

Fig. 9. Test Setup

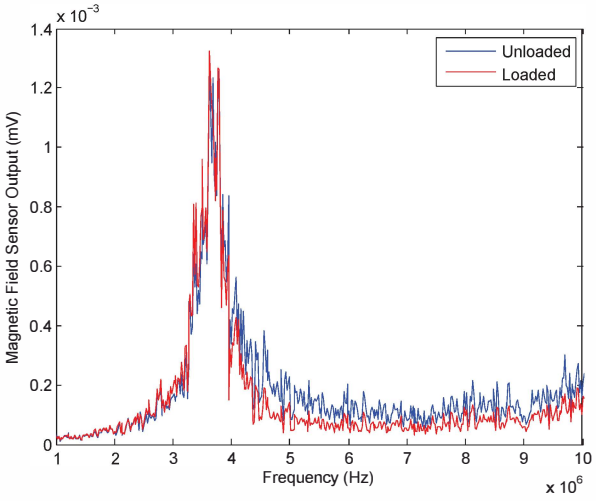

Fig. 10. Test Spectra from Loaded and Unloaded Secondary Driven By A Two-Quadrant Spread Sequence.

amplifiers use EPC2012 GaN devices with an output voltage that is nominally 100 V.

The magnetic field spectrum in Fig. 10 is measured from a fixed distance by a Beehive Electronics 100A probe into the spectrum analyzer input of an Tektronix MDO4054-3 set at a resolution bandwidth of 10 kHz.

VIII. Conclusion

A spread spectrum approach to reducing electromagnetic interference from wireless power transfer systems was presented. The system uses spread spectrum sequences that are optimized for the hardware using genetic algorithms. The voltage on the transmitting inductor is modulated based on a variant of minimum shift keying, which allows a four-quadrant D^{-1}amplifier to operate with zero voltage switching. The wireless power is captured by a high order bandpass rectifier that is optimized using a surrogate model to alleviate the computation cost of performing time domain simulations.

ACKNOWLEDGMENT

The authors would like to thank Arthur H. Chang for his invaluable help. This work was supported by the Grainger Foundation.

REFERENCES

[1] K. A. Grajski, R. Tseng, and C. Wheatley, "Loosely-coupled wireless power transfer: Physics, circuits, standards," in *Microwave Workshop Series on Innovative Wireless Power Transmission: Technologies, Systems, and Applications (IMWS), 2012 IEEE MTT-S International*, 10-11 May 2012 2012, pp. 9–14.

[2] F. Minfan, Z. Tong, Z. Xinen, and M. Chengbin, "A 13.56 mhz wireless power transfer system without impedance matching networks," in *Wireless Power Transfer (WPT), 2013 IEEE*, 15-16 May 2013 2013, pp. 222–225.

[3] R. Tseng, B. von Novak, S. Shevde, and K. A. Grajski, "Introduction to the alliance for wireless power loosely-coupled wireless power transfer system specification version 1.0," in *Wireless Power Transfer (WPT), 2013 IEEE*, 15-16 May 2013 2013, pp. 79–83.

[4] J. Nadakuduti, L. Lin, and P. Guckian, "Operating frequency selection for loosely coupled wireless power transfer systems with respect to rf emissions and rf exposure requirements," in *Wireless Power Transfer (WPT), 2013 IEEE*, 15-16 May 2013 2013, pp. 234–237.

[5] A. S. Y. Poon, S. O'Driscoll, and T. H. Meng, "Optimal frequency for wireless power transmission into dispersive tissue," *Antennas and Propagation, IEEE Transactions on*, vol. 58, no. 5, pp. 1739–1750, 2010.

[6] A. Swerdlow, *Exposure to high frequency electromagnetic fields, biological effects and health consequences (100 kHz-300 GHz)*. International Commission on Non-Ionizing Radiation Protection, 2009.

[7] Y. Yamanaka and A. Sugiura, "Possible emc regulations for wireless power transmission equipment," in *Microwave Workshop Series on Innovative Wireless Power Transmission: Technologies, Systems, and Applications (IMWS), 2011 IEEE MTT-S International*, 12-13 May 2011 2011, pp. 97–100.

[8] D. Gonzalez, J. Balcells, A. Santolaria, J. C. Le Bunetel, J. Gago, D. Magnon, and S. Brehaut, "Conducted emi reduction in power converters by means of periodic switching frequency modulation," *Power Electronics, IEEE Transactions on*, vol. 22, no. 6, pp. 2271–2281, 2007.

[9] A. M. Stankovic, G. C. Verghese, and D. J. Perreault, "Randomized modulation of power converters via markov chains," *Control Systems Technology, IEEE Transactions on*, vol. 5, no. 1, pp. 61–73, 1996.

[10] A. M. Stankovic, G. E. Verghese, and D. J. Perreault, "Analysis and synthesis of randomized modulation schemes for power converters," *Power Electronics, IEEE Transactions on*, vol. 10, no. 6, pp. 680–693, // 1995.

[11] K. B. Hardin, J. T. Fessler, and D. R. Bush, "Spread spectrum clock generation for the reduction of radiated emissions," in *Electromagnetic Compatibility, 1994. Symposium Record. Compatibility in the Loop., IEEE International Symposium on*, 22-26 Aug 1994 1994, pp. 227–231.

[12] C. Hsiang-Hui, I. H. Hua, and L. Shen-Iuan, "A spread-spectrum clock generator with triangular modulation," *Solid-State Circuits, IEEE Journal of*, vol. 38, no. 4, pp. 673–676, 2003.

[13] R. J. Gutmann and J. M. Borrego, "Power combining in an array of microwave power rectifiers," *Microwave Theory and Techniques, IEEE Transactions on*, vol. 27, no. 12, pp. 958–968, 1979.

[14] A. Ivascu, M. K. Kazimierczuk, and S. Birca-Galateanu, "Class e resonant low ¡e1¿dv¡/e1¿/¡e1¿dt¡/e1¿ rectifier," *Circuits and Systems I: Fundamental Theory and Applications, IEEE Transactions on*, vol. 39, no. 8, pp. 604–613, 1992.

[15] D. C. Jones and R. W. Erickson, "Analysis of switching circuits through incorporation of a generalized diode reverse recovery model into state plane analysis," *Circuits and Systems I: Regular Papers, IEEE Transactions on*, vol. 60, no. 2, pp. 479–490, 2013.

[16] M. Yelten, T. Zhu, S. Koziel, P. Franzon, and M. Steer, "Demystifying surrogate modeling for circuits and systems," *IEEE Circuits Syst. Mag.*, vol. 12, no. 1, pp. 45–63, 2012. [Online]. Available: http://ieeexplore.ieee.org/stamp/stamp.jsp?arnumber=6155115

[17] B. Liu, D. Zhao, P. Reynaert, and G. Gielen, "Gaspad: A general and efficient mm-wave integrated circuit synthesis method based on surrogate model assisted evolutionary algorithm," *IEEE Trans. Comput.-Aided Design Integr. Circuits Syst.*, vol. 33, no. 2, pp. 169–182, 2014. [Online]. Available: http://ieeexplore.ieee.org/stamp/stamp.jsp?arnumber=6714475

[18] S. Braun, T. Donauer, and P. Russer, "A real-time time-domain EMI measurement system for full-compliance measurements according to cispr 16-1-1," *IEEE Trans. Electromagn. Compat.*, vol. 50, no. 2, pp. 259–267, 2008. [Online]. Available: http://ieeexplore.ieee.org/stamp/stamp.jsp?arnumber=4506838

[19] G. Wang, W. Liu, M. Sivaprakasam, M. Zhou, J. Weiland, and M. Humayun, "A wireless phase shift keying transmitter with q-independent phase transition time," in *Engineering in Medicine and Biology Society, 2005. IEEE-EMBS 2005. 27th Annual International Conference of the*, 2005, pp. 5238–5241. [Online]. Available: http://ieeexplore.ieee.org/stamp/stamp.jsp?arnumber=1615660

[20] M. Cinteza, I. Marghescu, and T. Radulescu, "Design of PN sequence families with bounded correlation properties, using genetic algorithms," in *Computer as a Tool, 2005. EUROCON 2005.The International Conference on*, vol. 2, 2005, pp. 1818–1821. [Online]. Available: http://ieeexplore.ieee.org/stamp/stamp.jsp?arnumber=1630332

[21] S.-J. Chang, H.-S. Hou, and Y.-K. Su, "Automated passive filter synthesis using a novel tree representation and genetic programming," *IEEE Trans. Evol. Comput.*, vol. 10, no. 1, pp. 93–100, 2006. [Online]. Available: http://ieeexplore.ieee.org/stamp/stamp.jsp?arnumber=1583630

[22] V. Verma and B. Singh, "Genetic-algorithm-based design of passive filters for offshore applications," *IEEE Trans. Ind. Appl.*, vol. 46, no. 4, pp. 1295–1303, 2010. [Online]. Available: http://ieeexplore.ieee.org/stamp/stamp.jsp?arnumber=5462950

[23] A. V. Oppenheim, R. W. Schafer, J. R. Buck *et al.*, *Discrete-time signal processing*. Prentice-hall Englewood Cliffs, 1989, vol. 2.

[24] T. G. Kolda, R. M. Lewis, and V. Torczon, "Optimization by direct search: New perspectives on some classical and modern methods," *SIAM review*, vol. 45, no. 3, pp. 385–482, 2003. [Online]. Available: http://epubs.siam.org/doi/abs/10.1137/S003614450242889